

## **AN ANALYSIS OF JUNCTION DISCONTINUITY EFFECTS IN THE MULTI-ELEMENT COUPLED LINES AND ITS DIMINUTION AT DESIGNING STAGE**

**Rana Pratap Yadav<sup>\*</sup>, Sunil Kumar, and S. V. Kulkarni**

Institute for Plasma Research, Bhat, Gandhinagar 382428, India

**Abstract**—The analysis and design of the multi-element coupled lines, in conjunction with the junction discontinuity effect, is presented, and its applicability in high power rf regime is discussed. Junctions are usually employed to connect two different coupled elements, which gives rise to undesirable reactance, i.e., junction discontinuity effect. These effects are found prominent in the high power coupled lines for HF and VHF applications because of its large structural dimensions. The design and simulation of 3-element,  $8.34 \pm 0.2$  dB coupled line section rated for 38 to 112 MHz and 200 kW has been performed. The simulated results are significantly deviated from the theoretically calculated ones where the discontinuity effect is usually ignored. A generalized theoretical procedure is developed to take into account the effect of junction discontinuity at the designing stage. The theory is applied to the 3-element  $8.34 \pm 0.2$  dB coupled-line section, and simulation is performed by using standard Ansoft HFSS software. The HFSS simulation results are in close agreement with the theoretical predictions.

### **1. INTRODUCTION**

The multi-element coupled lines are used in the development of many components for rf and microwave systems such as balanced mixer, phase correlator, balanced amplifier, balanced modulator, attenuator, power measurements, antenna array networks. One of its most popular applications is the development of strip-line based 3 dB broadband hybrid coupler in HF and VHF range of frequencies. These 3 dB hybrid couplers are used as power combiner/divider or to protect the rf source by coupling the reflected power with the isolated port, i.e., terminated with the dummy load [1–3].

---

*Received 19 August 2013, Accepted 16 October 2013, Scheduled 23 October 2013*

\* Corresponding author: Rana Pratap Yadav (ranayadav97@gmail.com).

The hybrid coupler also has an application in tokamak plasma fusion research where rf power is introduced with the help of multiple coaxial transmission lines and antennae. Plasma load impedance continuously varies, because this rf power is reflected back to the generator, and at certain level it can damage the generator. In order to avoid the reflection, 3 dB hybrid coupler in certain configuration is used so that the reflected power is transmitted to the isolated port at which the dummy load is connected. The ion cyclotron resonance heating (ICRH) system of tokamak uses continuous wave radio frequency (cwrif) of 10 to 110 MHz and 100 kW onward (up to tens of MW). The ratings depend upon geometry of the tokamak, desired plasma parameters and toroidal magnetic field at the center of tokamak vessel. The broadband 3 dB hybrid coupler in ICRH system is used to divide the rf power coming from the source and to protect the rf source by coupling of reflected power with dummy load [4]. Single quarter-wavelength coupled-line based hybrid coupler works in narrow band of frequencies and has limited applications. The multi-octave bandwidth can be achieved by means of cascading several quarter-wavelength elements called multi-element coupler. In an earlier work, Cristal and Young [5] have given a theoretical approach for the designing of symmetrical TEM mode multi-element coupler. The theory leads to explicit expression for essential parameters, viz., even- and odd-mode impedances for the elements, and these are tabulated for the 3, 5, 7 and 9 elements coupled lines. The tabulated parameters have been theoretically obtained for several decades of bandwidth.

It is planned to develop a  $3 \pm 0.2$  dB hybrid coupler rated for 38 to 112 MHz and 200 kW using two  $8.34 \pm 0.2$  dB coupled-lines sections in tandem consisting of 3 cascaded elements in each section. Each element of 8.34 dB coupled section is designed with Cristal tabulated parameters and simulated by using Ansoft High Frequency Structure Simulator software (HFSS.14) of 14th version. To achieve the required  $8.34 \pm 0.2$  dB coupling, these three element are arranged in a certain configuration and connected through the coupled strip-line junction. The resulting structure is simulated again by using software HFSS. The simulated results are found significantly deviated from the calculated values based on Cristal theory of multi-element coupled line design. Cristal theory holds well for perfect design and yields ideal performance. However, the theory does not take into consideration the unavoidable junction discontinuity effect. The HFSS software takes into account all practical aspects including the effect of junction discontinuity. The junctions contribute to the reactance between various quarter-wavelength elements and therefore degrade the performance of the system. Although degradation in

return loss and isolation due to effect of discontinuity in coupled strip-line is reported [6–8] earlier, this effect on the coupling has not been considered yet. In general, compensation techniques are used after fabrication if junction discontinuity effects are not considered at designing stage. The method of compensation for discontinuities utilizes additional components such as capacitor and open stub [6–10]. Commercially available lumped high-power rf capacitors are large in size and lossy. Connecting shunt capacitor in coupled line affects the coupling, and therefore compensation is also needed in the coupling gap. If open stubs are used, high electric field exists on edges that may result in arcing. Thus, traditional approach is not suitable for the development of high power wide-band hybrid coupler.

The junction discontinuity effect depends on junction length in addition to even- and odd-mode impedances. The deviation becomes significant in the high-power application because of larger structural dimensions. The junction length can be extended up to  $\lambda/25$ , corresponding to center frequency, and hence the performance gets deteriorated at extremes of the frequency band. This necessitates the parametric evaluation of junction discontinuity effect in the device.

Here, we report a general theoretical procedure where an analytical equivalence of junction discontinuity effect is derived for the known junction parameters. The equivalent parameters of junction discontinuity effect are incorporated in Cristal theoretical design parameters for 3-element,  $8.34 \pm 0.2$  dB coupled line section. The coupling is calculated using standard procedure where the effect of junction discontinuity is included. In order to get an ideal performance, i.e., given by Cristal theory one needs to add compensation corresponding to junction discontinuity. In the process to verify the obtained results using modified theory (viz. cristal theory modified by restitution the effect of junction discontinuity effect), HFSS simulation is performed, and results are found in good agreement.

Section 2 describes the analysis of the coupled lines using Cristal parameters. Concept, design and simulation of the designed 3-element, 8.34 dB coupled-line section is explained in Section 3. Theory of junction discontinuity effect on multi-element coupled-line performance is given in Section 4. The modified theory for the multi-element coupled lines is illustrated in Section 5. Application of the modified theory in the design of 3-element,  $8.34 \pm 0.2$  dB coupled section is shown in Section 6. Results and discussion of the modified theory for the design and development of multi-element coupled line are discussed in Section 7, and conclusions are given in Section 8.

## 2. ANALYSIS OF COUPLED LINES

### 2.1. Single Element Coupled Line

The hybrid coupler shown in Figure 1 consists of two identical lines 1–2 and 3–4 with uniform electrical spacing over electrical length  $\theta$ . Here,

$$Z_{0e}Z_{0o} = Z_0. \quad (1)$$

where  $Z_{0e}$  and  $Z_{0o}$  represent the even- and odd-mode impedance of coupled lines. Signals emerging from the four ports can be given as [11]

$$\begin{aligned} A_1 &= \frac{1}{2} [\Gamma_{0e} + \Gamma_{0o}], \\ A_2 &= \frac{1}{2} [\Gamma_{0e} - \Gamma_{0o}], \\ A_3 &= \frac{1}{2} [T_{0e} + T_{0o}], \\ \text{and } A_4 &= \frac{1}{2} [T_{0e} - T_{0o}]. \end{aligned} \quad (2)$$

$A_1$ ,  $A_2$ ,  $A_3$  and  $A_4$  represent return loss, output, coupling and isolation of coupled lines where ports are terminated into matched load impedance. For the two-port network,  $\Gamma_{0e}$  and  $\Gamma_{0o}$  are the reflected wave amplitudes for the even and odd modes, respectively, while  $T_{0e}$  and  $T_{0o}$  are transmitted wave amplitudes for the even and odd modes, respectively.

The transmission coefficient  $T$  and reflection coefficient  $\Gamma$  are given by the following equation

$$\begin{aligned} \Gamma &= \frac{A_t + B_t - C_t - D_t}{A_t + B_t + C_t + D_t}, \\ T &= \frac{2}{A_t + B_t + C_t + D_t} \end{aligned} \quad (3)$$

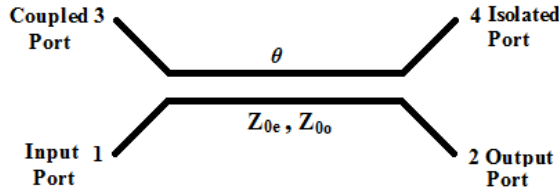


**Figure 1.** Schematic of quarter wave coupled section.

where,  $A_t$ ,  $B_t$ ,  $C_t$  and  $D_t$  are transmission matrix parameter of the coupled elements.  $\Gamma$  and  $T$  represent transmission and reflection coefficients. Using Equations (2) and (3),  $A_1$ ,  $A_2$ ,  $A_3$  and  $A_4$  for the matched coupled lines can be calculated as

$$\begin{aligned}
 A_1 &= 0, \\
 A_2 &= \frac{2}{2 \cos \theta + j (Z_{0e} + 1/Z_{0e}) \sin \theta}, \\
 A_3 &= \frac{j (Z_{0e} - 1/Z_{0e}) \sin \theta}{2 \cos \theta + j (Z_{0e} + 1/Z_{0e}) \sin \theta}, \\
 \text{and } A_4 &= 0.
 \end{aligned}
 \tag{4}$$

### 2.2. Coupled Line Section with Three Elements

Schematic diagram of the symmetrical 3-element coupler is shown in Figure 2 where extreme elements are identical. These three elements are named as  $B$ ,  $A$ ,  $B$ , where  $A_1$ ,  $A_2$ ,  $A_3$ ,  $A_4$  and  $B_1$ ,  $B_2$ ,  $B_3$ ,  $B_4$  are the return loss, output, coupling and isolation of element- $A$  and element- $B$ , respectively. To retain the perfect voltage standing wave ratio (VSWR) and isolation properties, each element has the same effective characteristic impedance.

$$\sqrt{Z_{0eA}Z_{0oA}} = \sqrt{Z_{0eB}Z_{0oB}} = 1.
 \tag{5}$$

where  $Z_{0eA}$ ,  $Z_{0eB}$  and  $Z_{0oA}$ ,  $Z_{0oB}$  are normalized even- and odd-mode impedances of element- $A$  and element- $B$ , respectively.

Initially, amplitude of emerging signal for each section is computed, and its combination for the multi-element coupler is solved using graphs network theory. The signal flow graph of the cascaded three coupled-elements are shown in Figures 3(a) and (b).

These two graphs are identical and represent the forward- and backward-wave propagation. In perfectly matched condition, port-4 is isolated ( $a_4 = 0$ ), and resulting signal flow graph is shown in Figure 4.

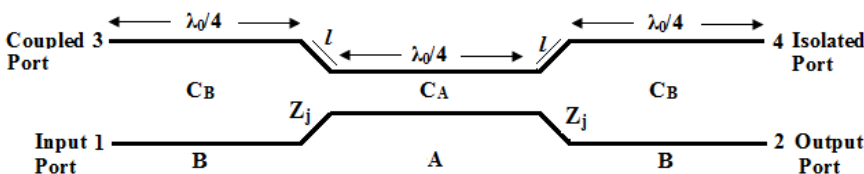
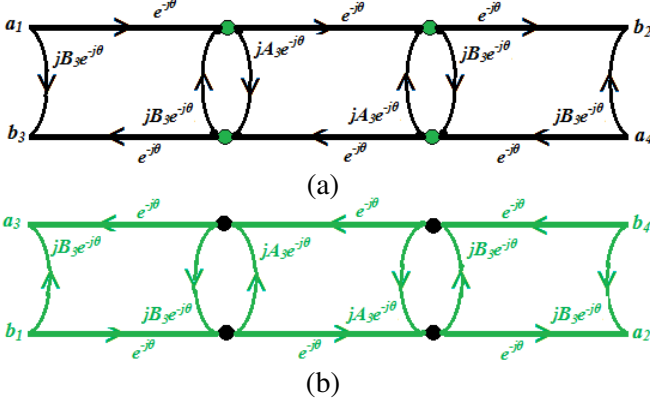
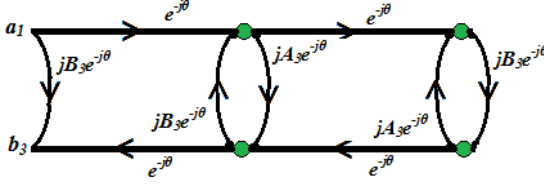


Figure 2. Schematic of 3-elements, 8.34 dB coupled line section.



**Figure 3.** Graphic representation of the 3-elements, 8.34 dB coupled line section. (a) Forward-wave, (b) backward-wave.



**Figure 4.** Reduced signal flow graph.

The coupled output  $b_3$  in terms of the incident wave  $a_1$  can be derived as follows,

$$\begin{aligned}
 b_3 &= jB_3 \cdot e^{-j\theta} + e^{-j\theta} \cdot jA_3 \cdot e^{-j\theta} \cdot e^{-j\theta} \\
 &\quad + e^{-j\theta} \cdot e^{-j\theta} \cdot jB_3 \cdot e^{-j\theta} \cdot e^{-j\theta} \cdot e^{-j\theta} \\
 &= jB_3 \cdot e^{-j\theta} + jA_3 \cdot e^{-j3\theta} + jB_3 \cdot e^{-j5\theta}. \quad (6)
 \end{aligned}$$

The overall coupling  $b_3$  of the three cascaded elements can be analyzed by making use of Equation (6) for the known coupling of element- $A$  and element- $B$ , i.e.,  $A_3$  and  $B_3$ .

The Cristal [5] table for  $8.34 \pm 0.2$  dB, 3-element coupled-lines section gives the normalized even-mode impedance for element- $A$  as  $Z_{0eA} = 1.7848$  and for element- $B$  as  $Z_{0eB} = 1.07434$ . Using these values in Equation (4),  $A_3$  and  $B_3$  are calculated. Now, the overall coupling  $b_3$  for  $8.34 \pm 0.2$  dB, 3-element coupled-lines section using Cristal tabulated parameter is analyzed and plotted using MATLAB software as shown in Figure 5. The result shown in Figure 5 represents the Cristal theoretical coupling for the  $8.34 \pm 0.2$  dB, 3-

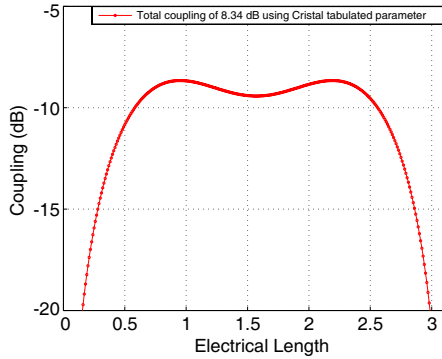


**Figure 5.** Characteristic of 3-elements, 8.34 dB coupled line section using Cristal theory, where coupling is plotted for 0 to  $\pi$ .

element coupled-lines section where the two extremes are equal and show ideal performance that one would like to achieve after fabrication of coupled-line section.

### 3. CONCEPT, DESIGN AND SIMULATION

In this section, the design and simulation of  $8.34 \pm 0.2$  dB coupled section rated for 38 to 112 MHz and 200 kW are presented. Multi-octave bandwidth can be achieved by means of cascading several quarter-wavelength elements called multi-element coupler. Coupling coefficient of the middle element is kept higher in proportion to the number of total element used in section. As the number of cascaded elements is increased, coupling gap of the middle element becomes narrow that reduces the power handling capability. Three elements namely *B*, *A* and *B* as shown in Figure 2 are designed to provide sufficient coupling gap which is essential for desired power rating.

Coupling coefficient of each element can be given by

$$C_A = \left( \frac{Z_{0eA}^2 - 1}{Z_{0eA}^2 + 1} \right) = \left( \frac{1 - Z_{0oA}^2}{1 + Z_{0oA}^2} \right) \quad (7)$$

$$C_B = \left( \frac{Z_{0eB}^2 - 1}{Z_{0eB}^2 + 1} \right) = \left( \frac{1 - Z_{0oB}^2}{1 + Z_{0oB}^2} \right). \quad (8)$$

From Cristal table  $Z_{0eA} = 1.7848$  and  $Z_{0eB} = 1.07434$  are used in Equation (7), and  $C_A = 0.5222$  and  $C_B = 0.07074$  are calculated corresponding to 6.123 dB and 22.896 dB, respectively. Dimensions of element-*A* and element-*B* are calculated for  $C_A$  and  $C_B$  by using known equations [4, 12, 13]. The coupled strip-line junctions are used

to join these elements for achieving  $8.34 \pm 0.2$  dB coupling and further simulated with HFSS software.

### 3.1. Simulation of the Designed Model Using HFSS

The model used for the simulation of the  $8.34 \pm 0.2$  dB coupled section consisting of 3-cascaded elements is shown in Figure 6. The rectangular strip-line central conductors are arranged in a particular configuration and placed in the grounded metallic enclosure of dimension  $310 \text{ cm} \times 60 \text{ cm} \times 12 \text{ cm}$ . Air within the grounded metallic enclosure is used as dielectric. The holding studs for the inner strip conductor and other transition, i.e., required for practical aspect, are avoided so that junction discontinuity effect can be analyzed independently. The length of each element is taken to be  $100 \text{ cm}$ , i.e., quarter wavelength at center frequency  $75 \text{ MHz}$ . For the given configuration, junction length of  $5 \text{ cm}$  is provided in each element. In the first step, the designed elements *A* and *B* are simulated independently, and their coupling performances are shown in Figures 7 and 8. The illustrated performances are verified for calculated values of  $6.123 \text{ dB}$  and  $22.896 \text{ dB}$  at the center frequency.

In the next step,  $50 \Omega$  coupled strip-line junction is physically employed to connect these three elements to achieve  $8.34 \pm 0.2$  dB coupling, and the simulation is performed again. The simulated

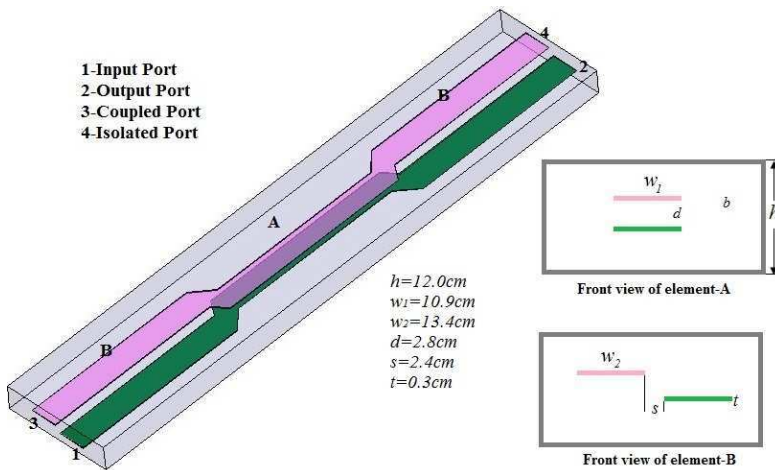


**Figure 6.** HFSS simulated model of 3-elements,  $8.34 \text{ dB}$  coupled line section.

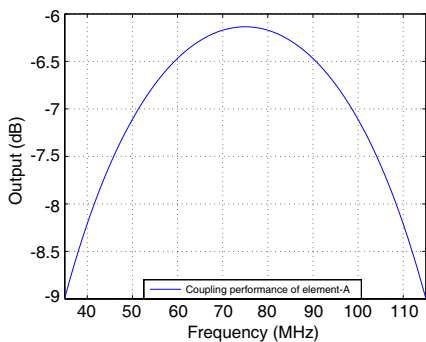


**Figure 7.** Using HFSS simulated coupling of element-A.

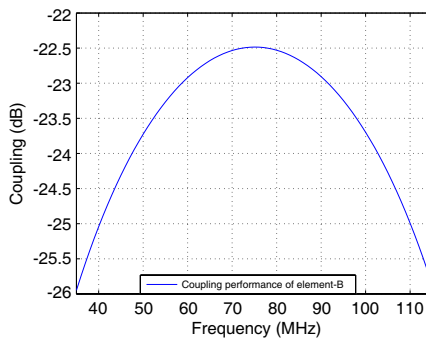


**Figure 8.** Using HFSS simulated coupling of element-B.

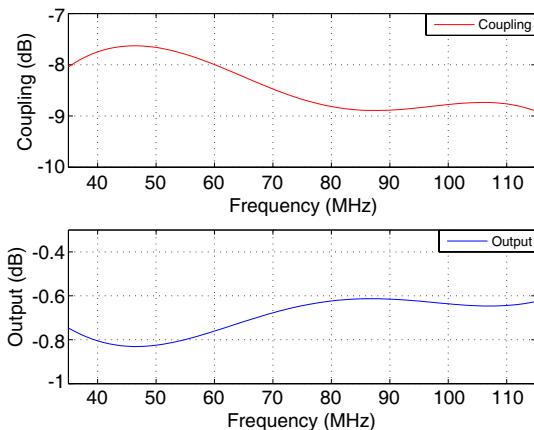


**Figure 9.** Using HFSS simulated performance of 3-elements, 8.34 dB coupled line section.

coupling and output performances are illustrated in Figure 9.

As explained in the previous section, both the maxima of the coupling or output parameters should be equal in the prescribed bandwidth. In HFSS simulation results, both the maxima at upper and lower ends of the frequency band are found unequal, and performances are significantly deteriorated from the theoretical prediction. This anomaly does not exist in case of element-A and element-B since the simulated couplings are in close agreement to calculated values. This attributes to the reactive effect of junction discontinuity.

#### 4. THEORY OF JUNCTION DISCONTINUITY

The coupled lines have always characterized by their even- and odd-mode behavior. The even- and odd-mode analysis of the junction along with element-*A* and element-*B* has been performed. In this case, junction represents the coupled transition between element-*A* and element-*B*. The even- and odd-mode impedances of the junction are taken as

$$Z_{0eA} > Z_{j0e} > Z_{0eB}, \quad Z_{0oA} < Z_{j0o} < Z_{0oB}.$$

where,  $Z_{j0e}$  and  $Z_{j0o}$  represent the even- and odd-mode impedances of junction. Schematic of junction with coupled elements *A* and *B* is shown in Figure 10.

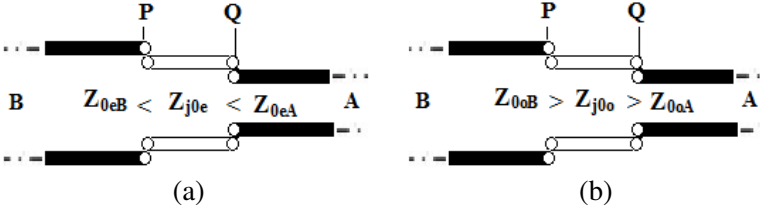


**Figure 10.** Schematic of junction between two coupled lines. (a) Even mode, (b) odd mode.

##### 4.1. Even Mode Analysis of Junction with Element-*A*

In Figure 10(a), input impedance at point-*Q*, i.e.,  $Z_{in(eAQ)}$  is given as

$$\begin{aligned} Z_{in(eAQ)} &= Z_{j0e} \frac{Z_{0eB} + jZ_{j0e} \tan \beta l}{Z_{j0e} + jZ_{0eB} \tan \beta l} \\ &\approx Z_{j0e} \frac{Z_{0eB} + jZ_{j0e} \beta l}{Z_{j0e} + jZ_{0eB} \beta l} \quad \text{for } \beta l \leq \pi/6. \end{aligned} \quad (9)$$

where,  $Z_{j0e} > Z_{0eB}$ ,  $l \leq \lambda/25$  and  $\beta l \ll 1$ , which implies  $Z_{0eB} \beta l \lll 1$ . Therefore,  $Z_{in(oAQ)}$  is approximated as,

$$Z_{in(eAQ)} \approx Z_{0eB} + jZ_{j0e} \beta l \quad (10)$$

Above analysis shows that junction discontinuity behaves as series inductance of  $Z_{j0e} \beta l / v$  with element-*A* in even mode.

Junction length  $l$  in terms of wavelength  $\lambda$  at center frequency  $f_0$  and arbitrary frequency  $f$  can be written as.

$$l = \frac{\lambda_0}{m_0} = \frac{\lambda}{m} \Rightarrow m = m_0 \left( \frac{f_0}{f} \right). \quad (11)$$

where  $m_0$  and  $m$  represent the wavelength to junction length ratio at  $f_0$  and  $f$ , respectively. Now, from Equations (10) and (11), inductive reactance  $jX_{jeA}$  due to junction with element- $A$  can be written as

$$jX_{jeA} = \frac{j2\pi Z_{j0e}}{m_0} \left( \frac{f}{f_0} \right) = \frac{j2\pi Z_{j0e}}{m_0} \left( \frac{\theta}{\theta_0} \right) = \frac{4jZ_{j0e}\theta}{m_0}. \quad (12)$$

where  $\theta$  and  $\theta_0 = \pi/2$  are the electrical lengths of the coupled element at variable frequency  $f$  and at center frequency  $f_0$ , respectively.

#### 4.2. Odd Mode Analysis of Junction with Element- $A$

From Figure 10(b), odd-mode admittance at point- $Q$ , i.e.,  $Y_{in(oAQ)}$  is given by,

$$Y_{in(oAQ)} = Y_{j0o} \frac{Y_{0oB} + jY_{j0o} \tan \beta l}{Y_{j0o} + jY_{0oB} \tan \beta l} \approx Y_{0oB} + jY_{j0o}\beta l. \quad (13)$$

where,  $Y_{j0o} > Y_{0oB}$  and  $\beta l \ll 1$ , which implies  $Y_{0oB}\beta l \lll 1$ .

From Equation (13), it can be noted that junction discontinuity behaves as shunt capacitance of  $Z_{j0e}l/v$  with element- $A$  in odd mode. The odd-mode admittance  $Y_{joA}$  at frequency  $f$  is derived as

$$jY_{joA} = \frac{j2\pi Y_{j0o}}{m_0} \left( \frac{f}{f_0} \right) \quad (14)$$

where  $Y_{j0o} = Z_{j0e}$  is put in Equation (14)

$$jY_{joA} = \frac{j2\pi Z_{j0e}}{m_0} \left( \frac{\theta}{\theta_0} \right) = \frac{4jZ_{j0e}\theta}{m_0} \quad (15)$$

From Equations (12) and (15), series inductance and shunt capacitance  $L_{jeA}$  and  $C_{joA}$  for the even and odd mode for the junction discontinuity are derived as.

$$L_{jeA} = C_{joA} = \frac{Z_{j0e}}{m_0 f_0} \quad (16)$$

Considering the junction discontinuity effect, the even and odd mode equivalence of element- $A$  has been shown in Figure 11.

Therefore, even- and odd-mode transmission matrix for element- $A$  is written as

$$\begin{bmatrix} A_{Ae'} & B_{Ae'} \\ C_{Ae'} & D_{Ae'} \end{bmatrix} = \begin{bmatrix} 1 & jX_{jeA} \\ 0 & 1 \end{bmatrix} \begin{bmatrix} \cos \theta & jZ_{0eA} \sin \theta \\ \frac{j \sin \theta}{Z_{0eA}} & \cos \theta \end{bmatrix} \begin{bmatrix} 1 & jX_{jeA} \\ 0 & 1 \end{bmatrix} \quad (17)$$

Considering  $Z_{0oA} = 1/Z_{0eA}$ , transmission matrix for odd mode is written as.

$$\begin{bmatrix} A_{Ao'} & B_{Ao'} \\ C_{Ao'} & D_{Ao'} \end{bmatrix} = \begin{bmatrix} 1 & 0 \\ jX_{joA} & 1 \end{bmatrix} \begin{bmatrix} \cos \theta & \frac{j \sin \theta}{Z_{0eA}} \\ jZ_{0eA} \sin \theta & \cos \theta \end{bmatrix} \begin{bmatrix} 1 & 0 \\ jX_{joA} & 1 \end{bmatrix}. \quad (18)$$

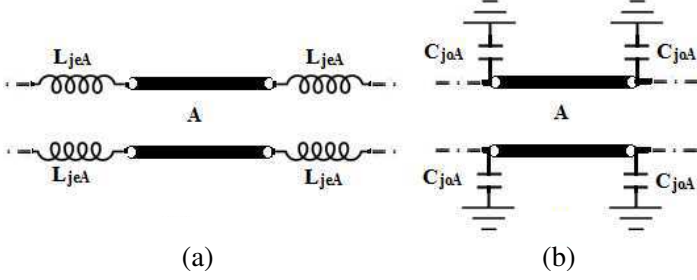


**Figure 11.** Equivalent circuit of the coupled element-*A*. (a) Even mode, (b) odd mode.

where  $A_{Ae'}$ ,  $B_{Ae'}$ ,  $C_{Ae'}$ ,  $D_{Ae'}$  and  $A_{Ao'}$ ,  $B_{Ao'}$ ,  $C_{Ao'}$ ,  $D_{Ao'}$  are the even- and odd-mode transmission matrix parameter of element-*A* including junction discontinuity effect.

Using Equations (17), (18) and (2), the emerging signals from the ports of element-*A* including junction is derived as.

$$\begin{aligned}
 A_{1'} &= 0, \\
 A_{2'} &= \frac{j \sin \theta \left( Z_{0eA} - \frac{1}{Z_{0eA}} \right) + j X_{jeA} \left( 2 \cos \theta - \frac{j X_{jeA} \sin \theta}{Z_{0eA}} \right)}{2 (1 - j X_{jeA}) \cos \theta - j \left( Z_{0eA} - \frac{1}{Z_{0eA}} (1 + j X_{jeA})^2 \right)}, \\
 A_{3'} &= \frac{2}{2 (1 - j X_{jeA}) \cos \theta - j \left( Z_{0eA} + \frac{1}{Z_{0eA}} (1 + j X_{jeA})^2 \right)}
 \end{aligned} \quad (19)$$

and  $A_{4'} = 0$ .

where,  $A_{1'}$ ,  $A_{2'}$ ,  $A_{3'}$  and  $A_{4'}$  are return loss, output, coupling and isolation of element-*A* including the effect of junction discontinuity.

### 4.3. Even Mode Analysis of Junction with Element-*B*

The junction discontinuity effect with element-*B* is also analyzed using the same procedure as that for element-*A*. As shown in Figure 10(a), input admittance at point-*P*, i.e.,  $Y_{in(eBP)}$ , is given as

$$\begin{aligned}
 Y_{in(eBP)} &= Y_{j0e} \frac{Y_{0eA} + j Y_{j0e} \tan \beta l}{Y_{j0e} + j Y_{0eA} \tan \beta l} \\
 &\approx Y_{j0e} \frac{Y_{0eA} + j Y_{j0e} \beta l}{Y_{j0e} + j Y_{0eA} \beta l} \quad \text{for } \beta l \leq \pi/6.
 \end{aligned} \quad (20)$$

where,  $Y_{j0e} > Y_{0eA}$ ,  $l \leq \lambda/25$  and  $\beta l \ll 1$ , which implies  $Y_{0eA}\beta l \lll 1$ . Therefore,  $Y_{in(eBP)}$  is approximated as,

$$Y_{in(eBP)} \approx Y_{0eA} + jY_{j0e}\beta l. \quad (21)$$

Therefore, junction discontinuity in even mode behaves as shunt capacitance with element- $B$ . The shunt admittance  $Y_{jeB}$  can be written as

$$jY_{jeB} = \frac{4j\theta}{m_0 Z_{j0e}}. \quad (22)$$

#### 4.4. Odd Mode Analysis of Junction with Element- $B$

In Figure 10(b), input impedance at point- $P$ , i.e.,  $Z_{in(eBP)}$ , is given as

$$\begin{aligned} Z_{in(eBP)} &= Z_{j0o} \frac{Z_{0oA} + jZ_{j0o} \tan \beta l}{Z_{j0o} + jZ_{0oA} \tan \beta l} \\ &\approx Z_{j0o} \frac{Z_{0oA} + jZ_{j0o}\beta l}{Z_{j0o} + jZ_{0oA}\beta l} Z_{0oA} + jZ_{j0o} \tan \beta l. \end{aligned} \quad (23)$$

where,  $Z_{j0o} > Z_{0oA}$ ,  $l \leq \lambda/25$  and  $\beta l \ll 1$ , which implies  $jZ_{0oA}\beta l \lll 1$ . Therefore,  $Z_{in(eBP)}$  is approximated as

$$Z_{in(eBP)} \approx Z_{0oA} + jZ_{j0o}\beta l. \quad (24)$$

Therefore, junction discontinuity in odd mode behaves as series inductance with element- $B$ . The series reactance  $X_{joB}$  is derived as

$$jX_{joB} = \frac{4j\theta}{m_0 Z_{j0e}}. \quad (25)$$

From Equations (22) and (25), the series inductance and shunt capacitance due to junction discontinuity are derived as

$$L_{joB} = C_{jeB} = \frac{1}{m_0 Z_{j0e} 1 f_0}. \quad (26)$$

where,  $L_{joB}$  and  $C_{jeB}$  are inductance and capacitance in odd and even mode with element- $B$  due to junction discontinuity. The equivalent circuit of element- $B$  with junction discontinuity effect is given in Figure 12.

Therefore, even- and odd-mode transmission matrix for element- $B$  can be written as

$$\begin{bmatrix} A_{Be'} & B_{Be'} \\ C_{Be'} & D_{Be'} \end{bmatrix} = \begin{bmatrix} 1 & jY_{j0eB} \\ 0 & 1 \end{bmatrix} \begin{bmatrix} \cos \theta & jZ_{0eB} \sin \theta \\ \frac{j \sin \theta}{Z_{0eB}} & \cos \theta \end{bmatrix} \begin{bmatrix} 1 & jY_{j0eB} \\ 0 & 1 \end{bmatrix}. \quad (27)$$

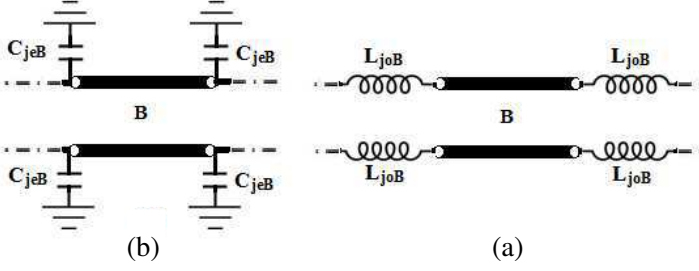


**Figure 12.** Equivalent circuit of element- $B$ . (a) Even mode, (b) odd mode.

Considering  $Z_{0oB} = 1/Z_{0eB}$  transmission matrix for odd mode is written as

$$\begin{bmatrix} A_{Bo'} & B_{Bo'} \\ C_{Bo'} & D_{Bo'} \end{bmatrix} = \begin{bmatrix} 1 & 0 \\ jX_{j0eB} & 1 \end{bmatrix} \begin{bmatrix} \cos \theta & \frac{j \sin \theta}{Z_{0eB}} \\ jZ_{0eB} \sin \theta & \cos \theta \end{bmatrix} \begin{bmatrix} 1 & 0 \\ jX_{j0eB} & 1 \end{bmatrix}. \quad (28)$$

where  $A_{Be'}$ ,  $B_{Be'}$ ,  $C_{Be'}$ ,  $D_{Be'}$  and  $A_{Bo'}$ ,  $B_{Bo'}$ ,  $C_{Bo'}$ ,  $D_{Bo'}$  are the even- and odd-mode transmission matrix parameters of element- $B$  including the effect of junction discontinuity.

The amplitude and phase of emerging signals from the ports of element- $B$  by using Equations (27), (28) and (3) are derived as

$$\begin{aligned} B_{1'} &= 0, \\ B_{2'} &= \frac{j \sin \theta \left( Z_{0eB} - \frac{1}{Z_{0eB}} \right) + jY_{j0eB} \left( 2 \cos \theta - \frac{jY_{j0eB} \sin \theta}{Z_{0eB}} \right)}{2(1 - jY_{j0eB}) \cos \theta - j \left( Z_{0eB} - \frac{1}{Z_{0eB}} (1 + jY_{j0eB})^2 \right)}, \\ B_{3'} &= \frac{2}{2(1 - jY_{j0eB}) \cos \theta - j \left( Z_{0eB} + \frac{1}{Z_{0eB}} (1 + jY_{j0eB})^2 \right)} \end{aligned} \quad (29)$$

and  $B_{4'} = 0$ .

where,  $B_{1'}$ ,  $B_{2'}$ ,  $B_{3'}$  and  $B_{4'}$  are return loss, output, coupling and isolation of element- $B$  including the effect of junction discontinuity.

By using Equation (6), amplitude of coupling for 3-element, 8.34 dB coupled line section including junction discontinuity effect is written as

$$b_{3'} = jB_{3'} \cdot e^{-j\theta} + jA_{3'} \cdot e^{-j3\theta} + jB_{3'} \cdot e^{-j5\theta}. \quad (30)$$

Coupling for element- $A$ , element- $B$  and 3-element coupled-line section by using Equations (19), (29) and (30) are plotted using MATLAB and shown in Figures 13, 14 and 15.

From Figures 13, 14 and 15, one can conclude the following facts.

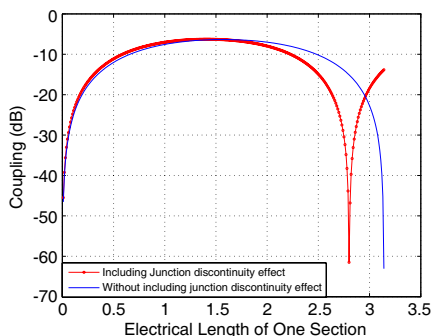


**Figure 13.** Calculated coupling of element-*A*.

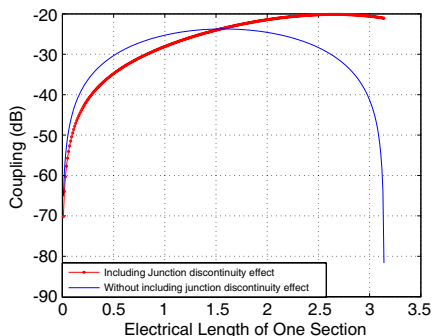


**Figure 14.** Calculated coupling of element-*B*.

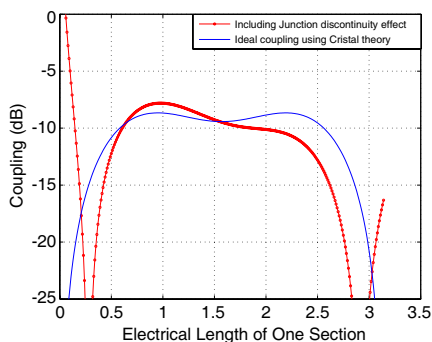


**Figure 15.** Calculated coupling of the 3-element,  $8.34 \pm 0.3$  dB coupled line section.

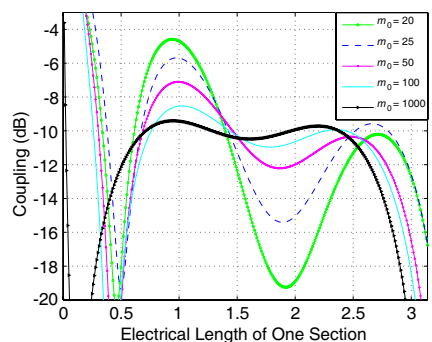


**Figure 16.** Coupling performance with varying junction length.

- (i) In Figure 13, after including the junction discontinuity effect, coupling of element-*A* increases to the left and decreases to the right of prescribed frequency band, where center frequency is shifted towards left with reduced frequency band.
- (ii) In Figure 14, after including the junction discontinuity effect, coupling of element-*B* decreases to the left and increases to the right of prescribed frequency band, where center frequency is shifted towards right with extended frequency band.
- (iii) The resultant effects of element-*A* and element-*B* are observed in coupling performance of 3-element,  $8.34 \pm 0.3$  dB coupled section.
- (iv) Coupling performance of  $8.34 \pm 0.3$  dB section is deviated from the Cristal theoretical results. The deviation is found of the same manner as simulated result shown in Figure 9.

The effect due to variation of junction length  $\lambda/m_0$  is shown in Figure 16. In this case, coupling of the designed 3-element,  $8.34 \pm 0.3$  dB coupled-line section is found increasing in the left half and decreasing in the right half from the calculated value. The deterioration depends on even- and odd-mode impedances of the junction. The deterioration may exist in the opposite manner if the choice of even- or odd-mode impedances for junction are within different boundary conditions. The above mentioned procedure can be followed in both the criteria. The magnitude of deterioration in coupling depends on the junction length. Therefore, junction length should be minimized.

## 5. MODIFIED THEORY OF COUPLED LINE DESIGN WITH JUNCTION DISCONTINUITY

The modified theory for the design of coupled lines including junction parameter is presented in this section. In the previous section, reactive behavior due to junction parameters is described which is to be taken into consideration at design stage. The superposition of the even and odd impedances of a coupled-lines is always constant and follows  $Z_{0e}Z_{0o} = 1$ . Therefore, the impedance matching of an element including junction can be made by modifying any one of the modes, which may be either even or odd mode.

### 5.1. Modification Used in Matching of Element-A

A small increment in the length of the quarter-wave coupled element behaves inductive in odd mode and capacitive in even mode whereas characteristic impedance remains the same. This fact may be utilized for the matching of element-A including junction. In the present case, length of element-A is increased to add capacitance in even mode so that the inductive effect of the junction discontinuity is countered. Schematic of element-A with the small increments in length  $\epsilon_A$  is shown in Figure 17.

In Figure 17, even-mode input admittance  $Y_{in(eR)}$  at point-R is given as

$$\begin{aligned} Y_{in(eR)} &= Y_{0eA} \frac{Y_0 + jY_{0eA} \tan(\pi/2 + \beta\epsilon_A)}{Y_{0eA} + jY_0 \tan(\pi/2 + \beta\epsilon_A)} \\ &= Y_{0eA} \frac{Y_0 + jY_{0eA} \cot \beta\epsilon_A}{Y_{0eA} + jY_0 \cot \beta\epsilon_A}. \end{aligned} \quad (31)$$

substituting characteristic admittance  $Y_0 = 1$ , we get

$$Y_{in(eR)} = Y_{0eA} \frac{1 - jY_{0eA} \cot \beta\epsilon_A}{Y_{0eA} - j \cot \beta\epsilon_A}$$

$$= Y_{0eA} \frac{\beta \epsilon_A - j Y_{0eA}}{Y_{0eA} \beta \epsilon_A - j} \quad \text{valid for the } \epsilon < \pi/6. \quad (32)$$

Now, it can be simplified as

$$Y_{in(eR)} = Y_{0eA}^2 \frac{\beta^2 \epsilon_A^2 + 1}{\beta^2 \epsilon_A^2 Y_{0eA}^2 + 1} + j Y_{0eA} \beta \epsilon_A \frac{1 - Y_{0eA}^2}{\beta^2 \epsilon_A^2 Y_{0eA}^2 + 1}. \quad (33)$$

Here,  $Y_{0eA} < 1$ ,  $\epsilon_A < 1$ ,  $\beta < 1$  gives  $Y_{0eA}^2 \beta^2 \epsilon_A^2 \lll 1$ . This gives,

$$Y_{in(eR)} = Y_{0eA}^2 + j \epsilon_A \beta Y_{0eA} (1 - Y_{0eA}^2). \quad (34)$$

This can also be written as

$$Y_{in(eR)} = \frac{Y_{0eA}^2}{Y_0} + \frac{j \epsilon_A \beta Y_{0eA} (1 - Y_{0eA}^2)}{Y_0}. \quad (35)$$

The above equation represents quarter wave admittance transformer with series inductance. This implies that a small increment in length of an element behaves as shunt capacitance of value  $\epsilon_A Y_{0eA} (1 - Y_{0eA}^2) / v$  in the even mode. In case of odd mode, impedance  $Z_{ineR}$  at point-R is given as

$$Z_{ineR} = Z_{0oA}^2 + j \beta \epsilon_A Z_{0oA} (1 - Z_{0oA}^2). \quad (36)$$

Thus, a small increment in length of an element behaves as series inductance of value  $\beta \epsilon_A Y_{0eA} (1 - Y_{0eA}^2) / v$  in odd mode. Series

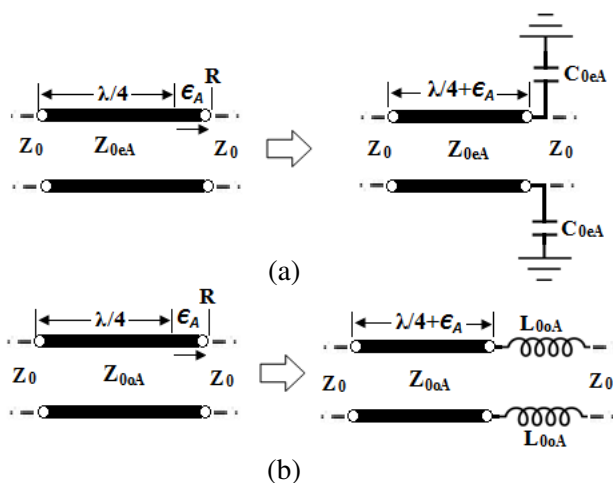


**Figure 17.** Schematic of the of element-A with small increments in length in (a) even mode, (b) odd mode.

inductance in odd mode and shunt capacitance in even mode for small increment in length of an element are found equal. Hence,

$$jY_{0eA} = jX_{0oA} = j\beta\epsilon_A Y_{0eA} (1 - Y_{0eA}^2). \quad (37)$$

The even and odd mode equivalence of the modified element-*A* along with the junction discontinuity effect has been shown in Figure 18.

From Figure 18, in matched condition one can write,

$$Z_{0eA} = \sqrt{\frac{X_{jeA}}{Y_{0eA}}}. \quad (38)$$

Value of  $\epsilon_B$  by using Equations (12) and (38) can be derived as

$$\epsilon_A = \frac{4Z_{0eA}Z_{j0e\theta}}{m_0\beta(Z_{0eA}^2 - 1)}. \quad (39)$$

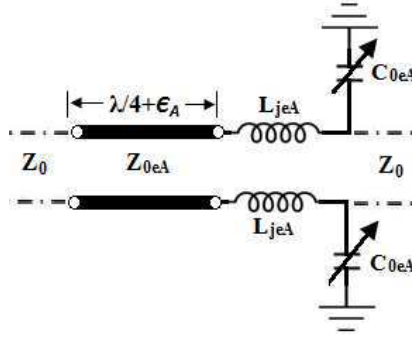


**Figure 18.** Matching of element-*A* by varying length.

## 5.2. Modification Used in Matching of Element-*B*

A small decrement in the length of the quarter-wave coupled element behaves capacitive in odd mode and inductive in even mode whereas characteristic impedance remains the same. This fact may be utilized for the matching of element-*B* including junction. In the present case, length of element-*B* is decreased to add inductance in even mode so that the capacitive effect of the junction discontinuity is countered. Schematic of element-*B* with the small decrement in length  $\epsilon_B$  is shown in Figure 19. In Figure 19(a), input admittance  $Y_{in(eS)}$  at point-*S* is given by

$$\begin{aligned} Y_{in(eS)} &= Y_{0eB} \frac{Y_0 + jY_{0eB} \tan(\pi/2 - \beta\epsilon_B)}{Y_{0eB} + jY_0 \tan(\pi/2 - \beta\epsilon_B)} \\ &\approx Y_{0eB} \frac{\beta\epsilon_B + jY_{0eB}}{Y_{0eB}\beta\epsilon_B + j} \quad \text{valid for the } \epsilon < \pi/6. \end{aligned} \quad (40)$$

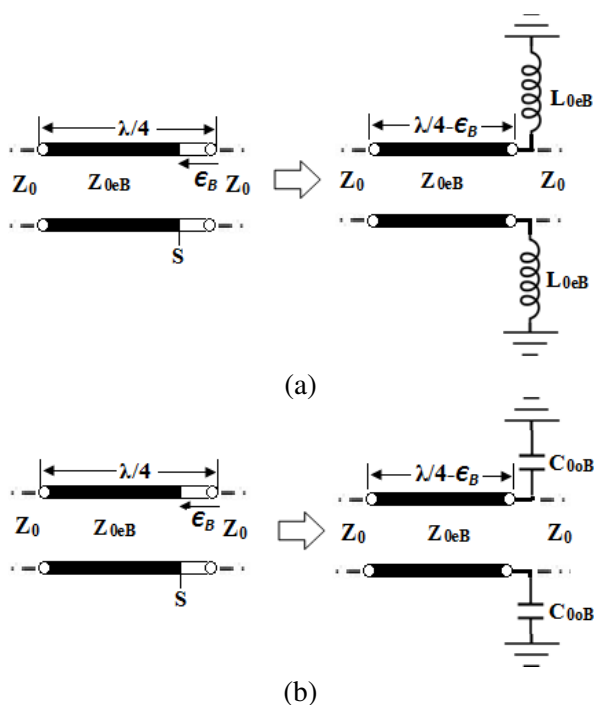


**Figure 19.** Schematic of the of element-*B* with small decrement in length. (a) Even mode, (b) odd mode.

Now, above equation is simplified as

$$Y_{in(eS)} = Y_{0eB}^2 \frac{\beta^2 \epsilon_B^2 + 1}{\beta^2 \epsilon_B^2 Y_{0eB}^2 + 1} + jY_{0eB} \beta \epsilon_B \frac{Y_{0eB}^2 - 1}{\beta^2 \epsilon_B^2 Y_{0eB}^2 + 1}. \quad (41)$$

Here,  $Y_{0eB} < 1$ ,  $\epsilon_B \ll 1$ ,  $\beta \ll 1$  gives  $Y_{0eB}^2 \beta^2 \epsilon_B^2 \ll 1$ . This gives

$$Y_{in(eS)} = Y_{0eB}^2 - j\beta \epsilon_B Y_{0eB} (1 - Y_{0eB}^2). \quad (42)$$

This also can be written as

$$Y_{in(eS)} = \frac{Y_{0eB}^2}{Y_0} - \frac{j\beta \epsilon_B Y_{0eB} (1 - Y_{0eB}^2)}{Y_0}. \quad (43)$$

The above equation represents quarter wave admittance transformer with series inductance. This implies that a small increment in length of an element behaves as shunt inductance of value  $1/\beta \epsilon_B Y_{0eB} (Y_{0eB}^2 - 1)v$  in the even mode. In case of odd mode, impedance  $Z_{inoS}$  at point-*S* is given as

$$Z_{inoS} = Z_{0oB}^2 - j\beta \epsilon_B Z_{0oB} (1 - Z_{0oB}^2). \quad (44)$$

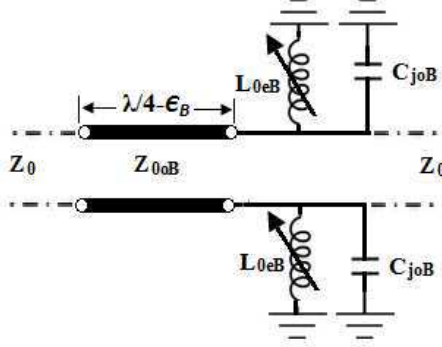


**Figure 20.** Matching of element- $B$  by varying length.

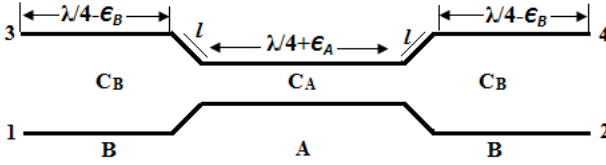


**Figure 21.** Schematic of the modified stepped 3-element coupled section.

Thus, a small decrement in length of an element behaves as series capacitance of value  $1/\beta\epsilon_B Z_{0oB}(1 - Z_{0oB}^2)v$  in odd mode. Series capacitance in odd mode and series inductance in even mode for a small decrement in length of an element are found equal. Hence,

$$jX_{0oB} = jY_{0eB} = j\beta\epsilon_B Z_{0oB} (1 - Z_{0oB}^2). \quad (45)$$

The even and odd mode equivalent to the modified element- $B$  along with the junction discontinuity effect is shown in Figure 20.

The junction discontinuity in even mode behaves as shunt capacitance  $C_{jeB1}$  with element- $B$  and decrease in length of element- $B$  adding inductance  $L_{0eB}$  to counter the junction discontinuity effect. In resonance condition

$$2\pi f \sqrt{L_{0eB} C_{jeB}} = \sqrt{X_{0oB} Y_{jeB}} = 1. \quad (46)$$

Value of  $\epsilon_B$  by using Equations (22) and (46) can be derived as

$$\epsilon_B = \frac{4\theta}{m_0 \beta Z_{j0e} Y_{0eB} (1 - Y_{0eB}^2)}. \quad (47)$$

The above analysis has been used for the design of a 3-element coupled-line section as shown in Figure 21. Modifications, i.e.,  $\epsilon_A$  and  $\epsilon_B$ ,

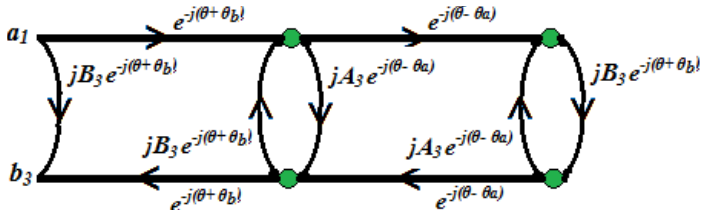


**Figure 22.** Reduced signal flow graph for the modified 3-element  $8.34 \pm 0.2$  coupled lines section.

are required in the length of element-A and element-B to counter the reactive effect of junction discontinuity.

From Figure 22, coupled signal  $b_{3m}$  for the modified 3-element coupled-line section can be written as

$$b_{3m} = jB_{3'} \cdot e^{-j(\theta + \theta_a)} + jA_{3'} \cdot e^{-j(3\theta + 2\theta_b - \theta_a)} + jB_{3'} \cdot e^{-j(5\theta + 3\theta_b - 2\theta_a)}. \quad (48)$$

where,  $\theta_a$  and  $\theta_b$  are electrical lengths corresponding  $\epsilon_A$  and  $\epsilon_B$  and given as

$$\theta_a = \beta \epsilon_a \quad \text{and} \quad \theta_b = \beta \epsilon_b. \quad (49)$$

## 6. APPLICATION OF MODIFIED THEORY IN DESIGN OF 3-ELEMENT, $8.34 \pm 0.2$ dB COUPLED SECTION

The  $8.34 \pm 0.2$  dB coupled section uses element-A and element-B of even-mode impedance  $Z_{0eA} = 1.7848$  and  $Z_{0eA} = 1.07434$ , i.e., normalized with  $Z_0 = 50 \Omega$ . The strip-line junctions of even-mode impedance  $Z_{j0e} = 1.312$  and length  $\lambda_0/80$  at center frequency 75 MHz are employed to connect element-A and element-B. By putting these values in Equations (47) and (39),  $\epsilon_A$  and  $\epsilon_B$  are calculated as

$$\epsilon_A = \frac{4 \times 1.71848 \times 1.312\theta}{80 \times \beta \times (1.71848^2 - 1)}.$$

where  $\theta = \theta_0 = \pi/2$  and  $\beta = 2\pi/\lambda_0$  at center frequency. That gives

$$\epsilon_A = \frac{4 \times 1.71848 \times 1.312 \times (\pi/2)}{80 \times (2\pi/\lambda_0) \times (1.71848^2 - 1)} = 0.014429\lambda_0.$$

Now,

$$\epsilon_B = \frac{4 \times (\pi/2)}{80 (2\pi/\lambda_0) \times 1.312 \times 0.93 \times (1 - 0.93^2)} = 0.07587\lambda_0.$$

Now making use of Equation (49),  $\theta_a$  and  $\theta_b$  can be calculated as

$$\theta_a = \left( \frac{2\pi}{\lambda} \right) (0.01342\lambda_0) = (2 \times 0.01342\pi) \left( \frac{\lambda_0}{\lambda} \right) = (0.02684\pi) \left( \frac{\theta}{\theta_0} \right)$$

using same procedure  $\theta_b = (0.14118\pi) \left( \frac{\theta}{\theta_0} \right)$ .

where  $\theta_0 = \pi/2$ . Using Equation (48),  $b_{3m}$  is calculated and plotted using MATLAB and is shown in Figure 23.

As shown in Figure 23, the coupling performance using modified theory is found in agreement to the ideal coupling using Cristal theory, which is desired where coupling including junction discontinuity effect is found much deviated. To verify the effectiveness of the modified theory, the calculated modification is incorporated in HFSS simulation model, and simulation is performed. The perspective comparison of coupling and output  $S$ -parameters obtained from the HFSS simulation and theoretically calculated parameters using modified theory is shown in Figures 24 and 25, where effectiveness of the modified theory is proven.

*Note: — Junction discontinuity effect is derived in terms of capacitance or inductance values. These derived values are also useful for the previous method, where junction discontinuities effect is compensated using capacitor or open stub. Therefore, junction discontinuity analysis is also useful for other available compensation techniques. Modified theory is a simple approach by which junction discontinuity effect can be compensated without increasing the structure complexity.*

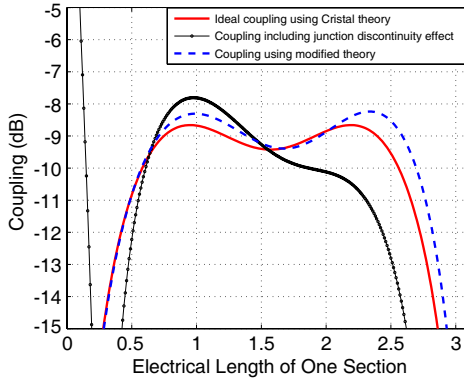


**Figure 23.** Comparison of the calculated coupling of the 3-element,  $8.34 \pm 0.3$  dB coupled line section using MATLAB.

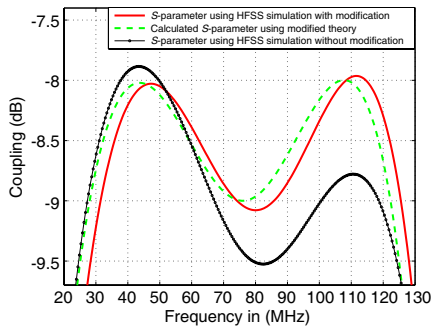


**Figure 24.** Comparison of coupling results obtained from HFSS simulation and modified theory.

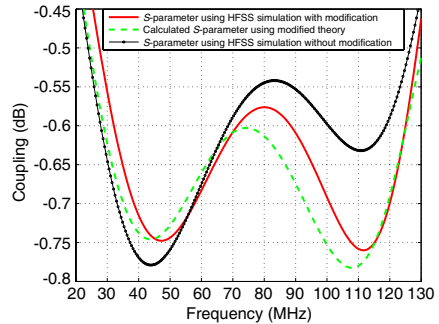


**Figure 25.** Comparison of output results obtained from HFSS simulation and modified theory.

## 7. RESULTS AND DISCUSSION

Junction discontinuity effect is comprehensively investigated while designing 3-element,  $8.34 \pm 0.2$  dB coupled-line section. Coupling and output  $S$ -parameters obtained from HFSS simulation are seen deviated from the expected results due to junction discontinuity effect. The left and right extremes in coupling performance are found 7.56 dB and 8.87 dB as shown in Figure 9 whereas its magnitude decreases continuously. This effect is also observed in the output  $S$ -parameters where magnitude is found increasing in the prescribed band. The left and right extremes of the output parameters are found  $-0.835$  dB and  $-0.63$  dB as shown in Figure 9. Both the maxima of the coupling and output  $S$ -parameters should be equal in the prescribed bandwidth whereas these are seen unequal due to the effect of junction discontinuity. The simulated coupling performance for element- $A$  and element- $B$  as shown Figures 7 and 8 are found in close agreement to the calculated values, i.e., 6.15 dB and 22.54 dB. This shows that element- $A$  and element- $B$  are perfectly designed. Therefore, undesirable effect of the junction discontinuities is confirmed.

A generalized theoretical procedure has been developed where analytical equivalence of junction discontinuity effect is derived for the known parameters. The equivalent of junction discontinuity parameter is incorporated into Cristal theoretical tabulated parameters for 3-element,  $8.34 \pm 0.2$  dB coupled-line section and coupling  $S$ -parameters are calculated as shown in Figure 15. The calculated left and right maxima of coupling parameter of 3-element coupled-line section are deviated from the Cristal theoretical results, and deviation is found in

the same manner as simulated results, shown in Figure 9.

To include the junction discontinuity parameter at the designing stage, a modified theory has been developed. The 3-element,  $8.34 \pm 0.2$  dB coupled-line section is designed by using modified theory, and the calculated results are shown in Figure 23. Both the maxima, i.e., approximately 8.25 dB, are found equal, and the result verifies the Cristal equal ripple theory outcomes. The software HFSS is used to simulate  $8.34 \pm 0.2$  dB coupled-line section, which is designed using modified theory. In simulated coupling performance as shown in Figure 24, left and right maxima are found 8.15 dB and 8.1 dB, respectively. In output performance, left and right maxima are found  $-0.74$  dB and  $-0.765$  dB, respectively, as shown in Figure 25. The HFSS simulation results are found in close agreement to expected results.

## 8. CONCLUSION

Junction discontinuity effect on multi-element coupled-lines performance and its diminution is presented using a novel theoretical approach. The reactive effect of junction discontinuity is derived and incorporated with even- and odd-modes analysis of the coupled element where the negative effect of junction discontinuity on  $S$ -parameters of 3-element coupled-lines section is presented and verified with the HFSS simulation result. In this theory, equivalent parameters of junction discontinuity effect for each of the elements are derived in terms of capacitance and inductance. The derived parameters are used in characterization of coupled elements independently where various aspects can be explored for compensation of this effect. This theory can also be generalized for  $n$ -element coupled-line section. Using the developed theoretical approach, junction parameters can be included in Cristal theory where tabulated even-mode impedances of coupled elements can be optimized for specified junction parameter. It is expected that the modified theory will help in the design of high power hybrid couplers.

## REFERENCES

1. Oliver, B. M., "Directional electromagnetic couplers," *Proc. IRE*, Vol. 42, 1688–1692, Nov. 1954.
2. Jemesand, E. M. T. and J. T. Bolljahn, "Coupled-strip transmission line filters and directional couplers,," *IRE Trans. Microw. Theory Tech.*, Vol. 4, 75–81, Apr. 1956.
3. Dydyk, M., "General synthesis of symmetric multi-element

- coupled transmission line directional couplers," *IEEE Trans. Microw. Theory Tech.*, Vol. 47, No. 6, 956–964, Jun. 1999.
4. Yadav, R. P., S. Kumar, and S. V. Kulkarni, "Design and development of 3 dB patch compensated tandem hybrid coupler," *Rev. Sci. Instrum.*, Vol. 84, 014702, 2013.
  5. Cristal, E. G. and L. Young, "Theory and table of optimum symmetrical TEM-mode coupled transmission line directional coupler," *IEEE Trans. Microw. Theory Tech.*, Vol. 13, No. 5, 544–553, 1965.
  6. Nakajima, M., E. Yamashita, and M. Asa, "New broadband 5-section microstrip-line directional coupler," *IEEE MTT-S Int. Microw. Symp. Dig.*, 383–386, 1990.
  7. Person, C., J. P. Coupez, S. Toutain, and M. Morvan, "Wideband 3-dB/90 coupler in multilayer thick-film technology," *Electron. Lett.*, Vol. 31, No. 10, 812–813, May 1995.
  8. Person, C., L. Carre, E. Rius, J. P. Coupez, and S. Toutain, "Original techniques for designing wideband 3-D integrated couplers," *IEEE MTT-S Int. Microw. Symp. Dig.*, 119–122, 1998.
  9. Kats, B. M., V. P. Meschanov, and A. L. Khvalin, "Synthesis of superwide-band matching adapters in round coaxial lines," *IEEE Trans. Microw. Theory Tech.*, Vol. 49, No. 3, 575–579, Mar. 2001.
  10. Gruszczynski, S., K. Wincza, and K. Sachse, "Design of compensated coupled stripline 3 dB directional couplers, phase shifters, and magic-T's," *IEEE MTT*, Vol. 54, No. 9, 3501–3507, 2006.
  11. Reed, J. and G. J. Wheeler, "A method of analysis of symmetrical four port networks," *IRE Trans. Microw. Theory Tech.*, Vol. 4, 246–252, Oct. 1956.
  12. Cohn, S. B., "Characteristic impedance of the broad-side coupled strip transmission line," *IRE Trans. Microw. Theory Tech.*, Vol. 8, 633–637, Nov. 1960.
  13. Bhat, B. and S. K. Koul, *Stripline-like a Transmission Lines for Microwave Integrated Circuit*, 138–139, 282–284, New Age International Publishers, India, 2007.